

Article

The Influence of Circular Physical Human–Machine Interfaces of Three Shoulder Exoskeletons on Tissue Oxygenation

Christine Linnenberg ^{1,*} , Benjamin Reimeir ^{1,2}, Robert Eberle ³ and Robert Weidner ^{1,4} 

- ¹ Chair for Production Technology, Institute for Mechatronics, Universität Innsbruck, Technikerstraße 13, 6020 Innsbruck, Austria; benjamin.reimeir@uibk.ac.at (B.R.); robert.weidner@hsu-hh.de (R.W.)
- ² Department of Sport Science, Universität Innsbruck, Fürstenweg 185, 6020 Innsbruck, Austria
- ³ Unit of Engineering Mathematics, Department of Mathematics, Universität Innsbruck, Technikerstraße 13, 6020 Innsbruck, Austria; robert.eberle@uibk.ac.at
- ⁴ Laboratory for Manufacturing Technology, Helmut-Schmidt-University/University of the Federal Armed Forces Hamburg, Holstenhofweg 85, 22043 Hamburg, Germany
- * Correspondence: christine.linnenberg@student.uibk.ac.at

Abstract: Occupational shoulder exoskeletons need to provide meaningful torques to achieve the desired support, thereby high pressures can occur within the physical human–machine interface (pHMI) of exoskeletons that may lead to discomfort, pain, or soft tissue injuries. This pilot study investigates the effects of occurring circumferential pressures within the pHMI in three different shoulder exoskeletons on the tissue oxygenation underneath the interfaces in resting position and dynamic use of the exoskeletons in 12 healthy subjects using near-infrared spectroscopy. Similar to standard Vascular Occlusion Tests, the tissue oxygen decreases while wearing the exoskeletons at rest (−2.1 (1.4) %/min). Dynamic use of the exoskeleton enhances the decrease in tissue oxygen (−7.3 (4.1) %/min) significantly and leads to greater resaturation after reopening the interface compared to resting position. This can be a sign of restricted blood supply to the upper extremity while wearing the exoskeleton. The shape and width of the circular interfaces showed no effect on the tissue oxygenation during use. Tissue oxygenation can be established as an additional safety criterion of exoskeletal pHMIs. The design of pHMI of shoulder exoskeletons should be reconsidered, e.g., in terms of open structures or the elasticity of closure straps to avoid occlusion effects.

Keywords: occupational exoskeleton; physical human–machine interface; circumferential compression; pressure; near infrared spectroscopy; TSI; muscle tissue oxygenation saturation; upper arm



Citation: Linnenberg, C.; Reimeir, B.; Eberle, R.; Weidner, R. The Influence of Circular Physical Human–Machine Interfaces of Three Shoulder Exoskeletons on Tissue Oxygenation. *Appl. Sci.* **2023**, *13*, 10534. <https://doi.org/10.3390/app131810534>

Academic Editor: João M. F. Rodrigues

Received: 28 June 2023
Revised: 28 August 2023
Accepted: 20 September 2023
Published: 21 September 2023



Copyright: © 2023 by the authors. Licensee MDPI, Basel, Switzerland. This article is an open access article distributed under the terms and conditions of the Creative Commons Attribution (CC BY) license (<https://creativecommons.org/licenses/by/4.0/>).

1. Introduction

Occupational exoskeletons were designed to reduce risk factors of work-related musculoskeletal disorders including heavy object manipulation, repetitive work, and non-ergonomic body postures [1]. They are targeted to carry, lift, and grip heavy loads, stabilize prone work postures, or allow sitting in any situation. Depending on their purpose, occupational exoskeletons are primarily designed to support one body region, e.g., back [2], shoulder [3], elbow [4], or hand [5].

Shoulder exoskeletons are specifically designed to support heavy and/or repetitive overhead tasks, such as assembly tasks in the automotive or aviation industry, drywall construction, picking and packing, or cleaning tasks by supporting arm motions against gravity with actuators. Recent studies have shown good potential to reduce physical demands [6–8], muscle fatigue [9], metabolic effects [10], and mental load [11] during tasks at head level or above.

Shoulder exoskeletons are mostly designed as backpack structures with a chest and pelvic harness and an additional kinematic structure with a physical human–machine interface (pHMI) (In the context of this article, HMI is not understood as a communication instrument including sensors or as part of a control circuit. It is rather a passive structural

element through which the user interacts with the machine (exoskeleton) by means of force transfer to the upper arm.) The vertical forces of the exoskeleton that support the lifting of the arms can be generated either passively (e.g., by springs and elastic elements) or actively (e.g., by electric motors or pneumatic systems) [12].

The main focus in the development process of shoulder exoskeletons is on reducing the weight of the exoskeleton, improving the kinematics including joint alignment [13] as well as the design of the physical human–machine interface [14].

Primarily, physical human–machine interfaces of exoskeletons have to fulfill two main requirements: (1) fixation of the exoskeleton to the body and thus enabling human control over the exoskeleton and (2) transferring the torques generated by the actuators to the user to assist in resting positions or during dynamic movements. Hence, the effectiveness of exoskeletons depends directly on the quality of the pHMI [15]. Currently, pHMIs of rigid shoulder exoskeletons are widely designed with a hard shell connected to the kinematic structure, padding, and a more or less elastic belt, which serves as a circular enclosure of the arm [16]. pHMIs of soft exoskeletons instead, largely go without hard materials. Since they follow a pull principle, soft materials such as neoprene usually form circular interfaces that can be adjusted in size with Velcro or similar [17,18].

pHMIs of exoskeletons in general are often associated with discomfort, pain, or soft tissue injuries [19–21]. To achieve the desired support, the exoskeletons need to provide meaningful external torques [22], especially when additional weight or heavy tools are carried. These torques can lead to very high pressures within the pHMI as well as the tissue underneath and may result in reduced blood supply to the tissue. The risk for soft tissue damage depends not only on the magnitude of pressure but also on its direction and distribution as well as on the duration and frequency of exposure, the integrity, tone, thickness, and mechanical stiffness of the tissue, and the proximity of bony prominences [21,23,24]. An adequate supply of blood is essential for the integrity of tissue.

In the case of shoulder exoskeletons and overhead work, it must be taken into account that blood flow in the elevated arm is already reduced [25]. Combined with high repetitive loads, this can result in several long-term upper extremity disorders such as musculoskeletal injuries or compression syndromes [26–30].

Since it is not possible to establish safe thresholds for soft tissue mechanical loading at the pHMI based on interfacial pressure measurements alone [31], this pilot study investigates tissue oxygenation as an additional physiological metric, thus focusing on the user safety in assessing the human–exoskeleton interaction. Near-infrared spectroscopy (NIRS) is a well-tolerated, non-invasive, and widely used technique for determining oxygen saturation and blood flow in the capillary bed of soft tissue. In terms of occupational exoskeleton evaluation, NIRS has mostly been used to detect muscle fatigue [32–34]. Another application of NIRS in recent exoskeleton studies is on human–machine interaction, prefrontal cortex activity, and muscle activation patterns, e.g., in exoskeleton-based rehabilitation after stroke [35,36].

To our knowledge, only two studies used NIRS concerning the evaluation of physical human–machine interfaces of exoskeletons [37,38]. Kermavnar et al. aimed to identify the impact of circumferential compression levels and different cuff sizes of a soft exoskeleton on the lower extremities during walking and directly related it to the occurrence of discomfort and pain. With regard to tissue oxygenation, (1) a negative correlation between inflation pressure and deep tissue oxygenation was found, (2) oxygen deprivation was differently tolerated at different sites of the lower extremity, and (3) the increase in oxygenation after cuff release differed at different sites in the lower extremity, which was further enhanced by a larger cuff.

To the authors' knowledge, there is no study to date that has utilized NIRS to measure tissue oxygenation in the upper extremity in the context of exoskeleton interface pressure. In a previous study, it was shown that pressure within shoulder exoskeleton pHMIs with a circular enclosure at the upper extremity exceeded the recommended pressure of 20 mmHg [39] by an average of ~23% in resting position (with the arm hanging) and by

an average of ~70% in dynamic arm movements [40]. However, to date, it has not been investigated how tissue oxygen saturation underneath the interface behaves during normal use of shoulder exoskeletons and whether exceeding the recommended pressures has a negative effect on tissue oxygenation. In addition, it is unclear whether the different designs of circular exoskeleton interfaces affect pressure and oxygen level.

Therefore, this pilot study investigates possible changes in muscle oxygenation saturation in the resting position and during dynamic overhead arm movements underneath the pHMI of three shoulder exoskeletons which were selected with respect to their pHMI design. This study investigates the following hypotheses:

- (i) pHMIs of shoulder exoskeletons restrict the blood supply underneath the pHMI and result in a decreased oxygen saturation in the soft tissue in resting posture.
- (ii) Dynamic arm movements with the shoulder exoskeletons have a neutralizing effect on the tissue oxygen saturation underneath the interface compared to resting conditions.
- (iii) The design of the pHMI influences the circumferential pressure and the tissue oxygenation underneath the pHMI.

2. Materials and Methods

2.1. Participants

A total of 12 male subjects were recruited from Innsbruck University. Informed consent was obtained from all subjects involved in the pilot study. Included were healthy male subjects 18 years of age or older who volunteered in the study. Subjects were excluded with the following criteria: (1) BMI > 30 kg/m²; (2) skinfold in the optodes area > 60% of the interoptode distance (21 mm); (3) cardiovascular, respiratory, neurological, or endocrine pre-existing diseases; (4) current musculoskeletal injury in the upper extremity area with acute or chronic pain; (5) local skin lesions in the optodes area; (6) ingestion of medications affecting cardiac, respiratory, neurological, or vasomotor system; (7) known allergic reactions to adhesives/patches. Subjects were instructed to observe the following: no food/alcohol/caffeine/nicotine 12 h prior to measurement, and no excessive exercise 24 h prior to testing. All subjects confirmed the absence of any exclusion criteria. All subjects completed the study protocol.

2.2. Physical Characteristics of the Participants

The physical characteristics of the subjects were recorded before the actual measurement (Table 1). These included blood pressure at rest, height, weight, upper arm circumference, and skinfold thickness in the area of the optodes (lateral head of triceps brachii). Systolic and diastolic blood pressure was measured in a seated position using a manual sphygmomanometer (Boso clinicus I, Bosch + Sohn, Jungingen, Germany). Skinfold thickness was obtained using a standard caliper (Bozeera, Dibb Trading B.V., Nijmegen, The Netherlands) and divided by 2 to determine adipose tissue thickness (ATT = fat + skin layer) [41]. Arm circumference was obtained using a standard cloth tape measure.

Table 1. Participants' characteristics.

Characteristics	Mean	SD	Unit
Age	29	1	yrs
Height	1.82	0.02	m
Weight	79	2.7	kg
Circumference of upper arm	29.5	1	cm
Skinfold thickness	3.5	0.6	mm
Systolic blood pressure	118.3	3.3	mmHg
Diastolic blood pressure	68.7	4.9	mmHg

2.3. Equipment

To assess the muscle oxygen saturation, the NIRS-System Porta-Lite (Artinis Medical Systems, Elst, The Netherlands) was applied underneath the human–machine interface of the exoskeleton at the height of the lateral head of the triceps brachii for data acquisition at 10 Hz. Changes in oxygenated (O_2Hb) and deoxygenated hemoglobin (HHb) can be obtained by applying the Lambert–Beer law, as the software (Oxysoft version 2.1.72, Artinis Medical Systems Netherlands) calculates changes in light absorption at different wavelengths (750 and 850 nm) and converts them to relative concentrations of O_2Hb and HHb. The optodes of this portable NIRS device have three transmitters and one receiver with an interoptode distance of 35 mm. This construction allows assessing the tissue oxygen saturation index (TSI; syn: $StO_2\%$, TOI; SmO_2 [42]) as an absolute value by using the spatial resolved spectroscopy method [43]. The path length factor was set to 4 for muscle investigations [44,45]. The device has a tissue penetration of about 18 mm, half the inter-uptode distance [41].

A custom-made pressure sensor was realized to measure the inner pressure of the physical pHMI of the exoskeletons (Figure 1). The device consists of a pressure pad ($3.5 \times 6.6 \times 0.3$ cm) obtained from a blood pressure cuff for infants (Bosch + Sohn GmbH (Boso), Jungingen, Germany), a piezoresistive silicon pressure sensor (Adafruit MPRLS Ported Pressure Sensor Breakout Board MPRLS0025Pa00001P, 0 to 25 PSI, Adafruit Industries, New York, USA) and a single-board computer (Raspberry Pi Zero W, Raspberry Pi Foundation, Cambridge, UK). Details and calibration data have been published previously [40]. The recording frequency was set to 10 Hz.

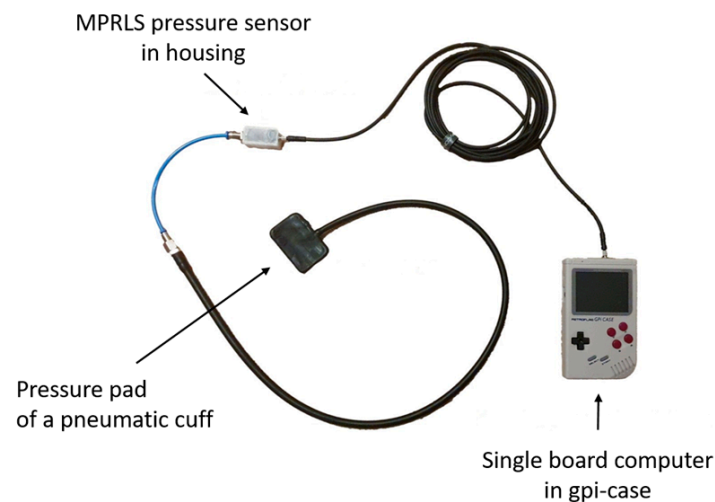


Figure 1. Custom-made pressure sensor.

2.4. Physical Human–Machine Interfaces

The physical human–machine interfaces of three exoskeletons were tested, all of which were designed for overhead work. In principle, all pHMIs were designed with a hard half-shell, padding and a quick-release buckle on an elastic belt, serving as a circular enclosure of the arm and enabling the control of the exoskeleton. They differ in form and width of the hard shells, thickness of paddings, and elasticity of the belts. Specific exoskeletons were (a) the Skelex 360 exoskeleton (Skelex), (b) the Lucy exoskeleton (Helmut-Schmidt-University), and (c) the Paexo Shoulder exoskeleton (Otto Bock); see Figure 2.

Technical data of the exoskeletons and their pHMIs can be found in Table 2. The exoskeletons studied were selected because they differ primarily in shape and width of the hard shells and padding, and thus enclose the arm circumference in varying degrees.



Figure 2. Exoskeletons and their pHMIs: (a) Skelex 360, (b) Lucy, and (c) Paexo Shoulder.

Table 2. Technical data of examined exoskeletons.

Exoskeleton	Institution	Type	Technology	pHMI Strap	pHMI Fixation	Weight	Support Force	pHMI Width × Length
Skelex 360	Skelex	Passive	Flex frame, spring	Elastic	Buckle	2.8 kg	up to 4.9 kg	13 × 22.5 cm
Lucy	HSU	Active	Air pressure	Elastic	Buckle	6.6 kg	up to 8 Nm	18 × 11.5 cm
Paexo Shoulder	Otto Bock	Passive	Mechanical pulley	Elastic	Buckle	1.9 kg	n/s *	15 × 17 cm

* Not specified in the instruction manual of the manufacturer.

2.5. Vascular Occlusion Method

Standard Vascular Occlusion Tests (VOT) [46,47] were conducted using a pneumatic tourniquet with an arm cuff dimension of 53 × 14 cm. The cuff was placed at the upper arm approximately 2–3 cm above the epicondyles. Vascular occlusions were applied at 50 mmHg (Ven.Occ.) and 200 mmHg (Art.Occ.) for venous and arterial occlusion for 2 min, respectively.

During venous occlusion, O₂ is still consumed in the tissue. As venous blood drainage is no longer possible, O₂ saturation decreases and the TSI signal declines; see Figure 3. During arterial occlusion, venous blood drainage as well as arterial blood supply is blocked and the TSI signal drops. Immediately after the occlusion is removed, fresh blood is directed into the tissue, and O₂ saturation increases. After deflation, the TSI signal may temporarily rise above the baseline value, indicating a post-ischemic, hyperemic vasodilation [46]. The course of the TSI signal is less pronounced in venous occlusion in most cases.

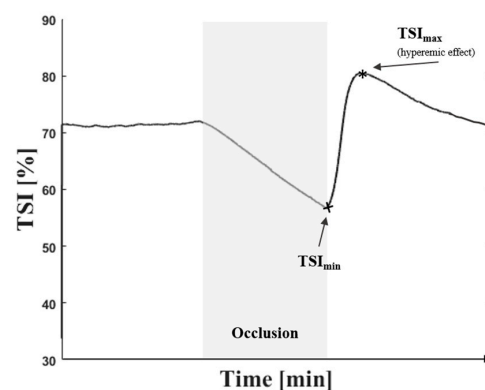


Figure 3. Response of tissue saturation index (TSI) to occlusion.

2.6. Testing Protocol

The testing protocol provided a total of eight measurements (Figure 4). After attaching the NIRS optodes and the pneumatic cuff, the test subject had to rest in a half-supine position for 15 min, a standard procedure before VOT tests [48]. Two standard VOTs with 50 mmHg and 200 mmHg were conducted standing using an automatic pneumatic tourniquet.

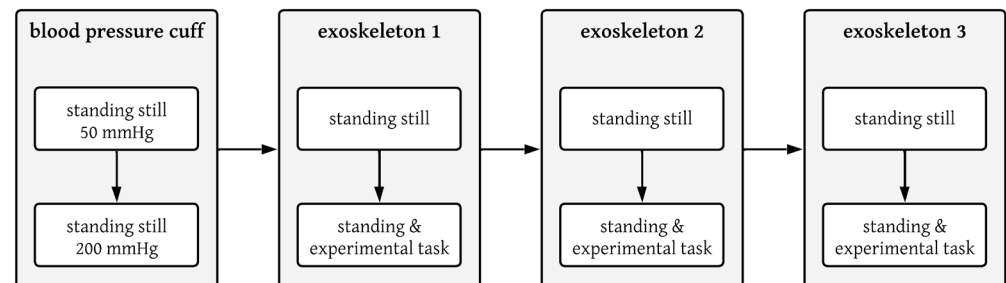


Figure 4. Schematic diagram of the testing protocol.

Measurements with the exoskeleton followed in random order. The exoskeleton was first attached and adjusted to the subject according to the manufacturers' specifications. The support was set to the maximum allowable level according to the specific manufacturer's specifications in relation to the user's weight and height. The pHMI was fitted in such a way that the wearer perceived the pHMI pressure as comfortable and could control the exoskeleton properly at the same time, as the wearer would do in normal use of the exoskeleton. The pHMI was opened again and a seated rest of at least 10 min followed to ensure that the oxygen level returned to baseline.

Similar to the standard VOT with the pneumatic cuff, in the exoskeleton test condition at rest, the subject stood still for the whole trial. NIRS measurement was started with a 2 min phase to record the TSI baseline. Then, the pHMI was closed by the investigator, lasting 2 min. After reopening the pHMI, the NIRS measurement ran for another 2 min to record any hyperemic effects and the return to baseline.

The second trial with the same exoskeleton was conducted to be equal in process to the first one. Only in the 2 min occlusion period, when the pHMI was closed, the subject was asked to repeat the dynamic task (see Section 2.7 Dynamic Movement) at his own pace holding an electric drill, as an employee would do in real work conditions. The second trial was conducted to verify whether the effect of a possibly restricted blood supply when wearing the exoskeleton could be neutralized by moving the arm with the exoskeleton in a typical use case. All measurements were conducted in a standing position, as it was hardly possible to sit while wearing the exoskeletons. Between each exoskeleton measurement, a 10 min break was taken.

2.7. Dynamic Movement

In the dynamic task, a typical overhead assembly is simulated in which bolts are repetitively placed on a board above head height. In the starting position (Figure 5), the subject stood in front of the workpiece, which was at a height of 2.3 m. The feet were parallel and the arms hung loosely down. The participant held a commercially available electric drill (mass ≈ 1.5 kg) in the dominant test hand. As soon as the pHMI was closed, the participant repeatedly moved the cordless screwdriver up and back down to the starting position and started over again. The participant repeated the experimental task at his own pace for 2 min of occlusion.



Figure 5. Sequence of the dynamic task.

2.8. Data and Statistical Analyses

NIRS and pressure data were evaluated using MATLAB, version 9.10.0 (R2021a). The TSI signal as output by Oxysoft software (Version 3.2.72) was first smoothed using a Butterworth filter at the fourth-order and low-pass filter with a cut-off frequency of 0.2 Hz. Baseline TSI (TSI_{Base}), was calculated as the average of 30 s before cuff occlusion or pHMI occlusion, respectively (Figure 6). The downslope of the TSI signal (TSI_{Slope1}) was calculated between the beginning of occlusion and the minimum TSI value during occlusion [49] by a linear regression equation and served as a measure of the O_2 desaturation rate [42], whereas the upslope of the TSI signal (TSI_{Slope2}) immediately after deflation served as a measure of the O_2 resaturation rate. TSI_{Slope2} was calculated between the end of occlusion and the maximum TSI value after occlusion using the linear regression equation. $TSI_{Overshoot}$ was calculated as the delta between TSI_{Base} and the maximum value of the TSI signal after deflation or opening of the pHMI, respectively. Mean pressure of the pHMI was calculated as the mean pressure signal of the pressure sensor during the occlusion period.

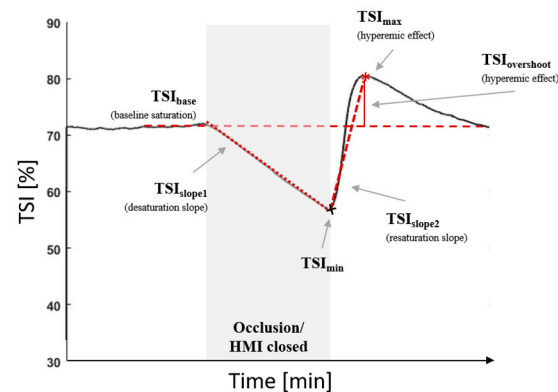


Figure 6. Illustration for the calculation of NIRS key outcome parameters.

All data were analyzed using IBM[®] SPSS Statistics Version 27. The significance level was set at $p < 0.05$. Mean pressure, TSI_{Slope1} , TSI_{Slope2} , and $TSI_{Overshoot}$ served as dependent variables. To address hypothesis no. (i) and (iii), “type of occlusion” was established as an independent five-step variable including arterial occlusion with pressure cuff, venous occlusion with pressure cuff, closed pHMI of the exoskeleton Lucy, closed pHMI of the exoskeleton Paexo Shoulder, and closed pHMI of Skelex 360. A repeated-measures ANOVA was performed, followed by pairwise comparisons with a Bonferroni correction of the alpha level to determine whether and which test modes differ from each other in resting position. In case of violation of sphericity, the correction according to Greenhouse–Geisser was used.

To determine the effect of movement versus resting position on oxygen levels (hypothesis (ii)), a two-factorial ANOVA was performed with the inner-subject factors’ “movement” (2): resting vs. dynamic condition and “pHMI design” (3): Lucy, Paexo Shoulder, and Skelex 360 for all aforementioned dependent variables.

3. Results

3.1. Pressure

pHMI pressure in the resting position conditions with exoskeletons averaged overall at 25.2 (14.4) mmHg, ranging from 6.6 to 59.3 mmHg. In the dynamic test condition with exoskeleton, pHMI pressure averaged overall at 40.3 (19.7) mmHg, ranging from 10.9 to 76.5 mmHg. Table 3 lists the mean and standard deviation pressure values for each of the exoskeletons and test conditions. All test conditions in resting posture differed significantly from arterial occlusion; see Table 3. Additionally, there was a significant difference in pHMI pressure for Lucy and Skelex 360 with venous occlusion condition, as well as a significant difference in pHMI pressure between Paexo and Lucy; see Table 4. The two-way ANOVA revealed a significant effect in movement as well as for pHMI design; compare Table 5.

Table 3. Descriptive data of the measurements (mean (standard deviation)).

	Resting Posture					Dynamic Movement		
	Art. Occ.	Ven. Occ.	Lucy	Paexo	Skelex	Lucy	Paexo	Skelex
Mean pressure [mmHg]	200.1 (1.8)	52.6 (0.4)	16.1 (6.5)	38.3 (14.3)	23.8 (11.8)	24.3 (12.9)	55.7 (21.4)	39.3 (10.7)
TSI _{Base} [%]	58.3 (3.1)	60.7 (2.8)	55.8 (8.0)	57.3 (6.3)	56.4 (5.8)	56.4 (6.9)	57.2 (5.3)	56.4 (5.9)
TSI _{Slope1} [%/min]	−2.1 (1.1)	−1.5 (0.5)	−1.6 (1.0)	−2.5 (2.2)	−2.7 (1.5)	−5.9 (3.6)	−9.0 (4.5)	−7.0 (4.3)
TSI _{Slope2} [%/min]	35.6 (18.4)	6.5 (5.7)	6.7 (5.9)	7.7 (5.9)	7.0 (5.5)	46.1 (33.3)	58.7 (25.4)	51.6 (36.8)
TSI _{Overshoot} [%]	9.8 (4.2)	−1.2 (2.7)	1.6 (2.7)	1.4 (1.7)	1.4 (2.4)	11.8 (6.4)	9.6 (5.7)	10.3 (5.8)

3.2. Tissue Oxygenation

TSI_{Base} averaged 57.2 (5.7) % for all test conditions before occlusion was applied or pHMI was closed. There was no significant difference in TSI_{Base} for all test conditions. Table 3 lists TSI_{Base} for each test condition.

Figure 7A shows the mean TSI trajectories of the test conditions in resting posture with closed exoskeleton interfaces against TSI trajectories of the standardized Vascular Occlusion Tests. Figure 7B shows the mean TSI trajectories of the dynamic exoskeleton conditions against the standard Vascular Occlusion Test trajectories.

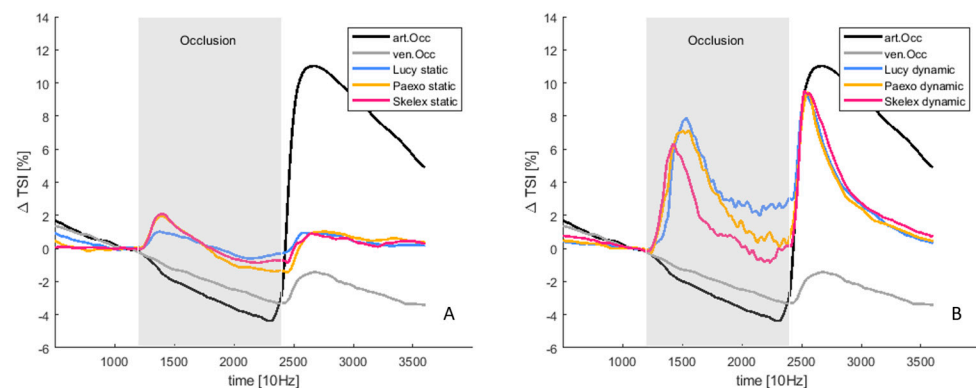


Figure 7. Mean TSI curves of VOTs and resting posture conditions (A) and dynamic conditions (B).

The downslope of TSI (TSI_{Slope1}) averaged −2.1 (1.4) %/min over all resting conditions. There was no significant difference between all resting conditions in TSI_{Slope1}; see Table 4. In dynamic test conditions, TSI_{Slope1} averaged −7.3 (4.1) %/min over all exoskeleton conditions. The TSI_{Slope1} values for each dynamic condition can be found in Table 3. The multifactorial ANOVA revealed a significant difference for TSI_{Slope1} between resting and dynamic test conditions (movement), whereas no significant difference was found for the exoskeleton design and the interaction between pHMI design and movement; compare Table 5.

Table 4. Repeated-measure ANOVA outcomes and post-hoc comparison for comparison of all resting conditions.

Outcome Parameter	Overall (p-Value (F-Value, η^2))	Sample 1	Sample 2	Distance	p-Value	CI-95%		
Mean pressure [mmHg]	<0.001 (767.32, 0.991) *	Art.Occ.	Ven.Occ.	147.550	<0.001 *	[144.5–150.5]		
			Lucy	184.499	<0.001 *	[179.7–179.7]		
			Paexo	160.019	<0.001 *	[140.2–179.7]		
			Skelex	176.848	<0.001 *	[160.1–193.5]		
		Ven.Occ.	Lucy	36.949	<0.001 *	[27.2–46.6]		
			Paexo	12.469	0.437	[−7.9–32.9]		
			Skelex	29.298	<0.001 *	[14.3–44.2]		
		Lucy	Paexo	24.480	0.006 *	[−41.2–−7.7]		
			Skelex	−7.6	0.427	[−20.1–4.8]		
		Paexo	Skelex	16.829	0.204	[−5.8–39.5]		
		TSI _{Slope1}	0.124 (1.984, 0.221)					
		TSI _{Slope2}	0.002 (13.194, 0.653) *	Art.Occ.	Ven.Occ.	27.985	0.022 *	[3.9–52.0]
Lucy	29.679				0.084	[−3.9–62.6]		
Paexo	28.838				0.042 *	[1.0–56.6]		
Skelex	26.134				0.054	[−0.3–52.6]		
Ven.Occ.	Lucy			1.694	1.000	[−11.6–14.9]		
	Paexo			0.853	1.000	[−9.7–11.4]		
	Skelex			−1.851	1.000	[−15.8–12.1]		
Lucy	Paexo			−0.841	1.000	[−10.5–8.8]		
	Skelex			−3.545	1.000	[−16.6–9.5]		
Paexo	Skelex			−2.704	1.000	[−10.4–4.6]		
TSI _{Overshoot}	<0.001(17.710, 0.717) *			Art.Occ.	Ven.Occ.	11.541	0.004 *	[4.1–18.8]
					Lucy	9.328	0.011 *	[2.2–16.4]
		Paexo	8.545		0.032 *	[0.7–16.3]		
		Skelex	8.9		0.014 *	[1.8–16.1]		
		Ven.Occ.	Lucy	−2.2	1.000	[−8.4–4.5]		
			Paexo	−2.9	0.114	[−6.5–0.5]		
			Skelex	−2.5	1.000	[−8.3–3.0]		
		Lucy	Paexo	−0.782	1.000	[−5.8–4.3]		
			Skelex	−0.436	1.000	[−4.4–3.7]		
		Paexo	Skelex	0.436	1.000	[−3.3–4.1]		

* Significant outcome, $p < 0.05$.

The upslope of the oxygen level (TSI_{Slope2}) after reopening the tourniquet or pHMI averaged at 35.6 (18.4) %/min for arterial occlusion, at 6.5 (5.7) %/min for venous occlusion, at 6.7 (5.9) %/min for Lucy, at 7.7 (5.9) %/min for Paexo Shoulder, and at 7.0 (5.5) %/min for Skelex 360 in resting condition; see Table 3. Repeated-measures ANOVA for the resting conditions revealed a difference between arterial occlusion and venous occlusion as well as between arterial occlusion and Paexo Shoulder; see Table 4. There was no difference between venous occlusions and the exoskeleton conditions as well as among the exoskeletons. In dynamic conditions, TSI_{Slope2} averaged at 51.9 (31.4) %/min for all exoskeleton conditions. The multifactorial ANOVA revealed a significant difference for movement but not for pHMI design or the interaction of the two factors for the dependent variable TSI_{Slope2}; see Table 5.

Table 5. Results of multifactorial ANOVA with repeated measures (*p*-value (F-value, η^2)).

Outcome Parameter	pHMI Design	Movement	pHMI Design \times Movement
Mean pressure	0.002 (22.488, 0.882) *	<0.001 (35.522, 0.835) *	0.918 (0.086, 0.028)
TSI _{Slope1}	0.058 (3.408, 0.299)	<0.001 (28.561, 0.781) *	0.421 (0.914, 0.102)
TSI _{Slope2}	0.637 (0.464, 0.055)	0.001 (23.916, 0.749) *	0.818 (0.203, 0.025)
TSI _{Overshoot}	0.988 (0.012, 0.002)	<0.001 (25.951, 0.764) *	0.901 (0.100, 0.012)

* Significant outcome.

A hyperemic effect appeared as TSI_{Overshoot} in the arterial occlusion, Lucy, Paexo Shoulder, and Skelex condition with 9.8 (4.2) %, 1.6 (2.7) %, 1.4 (1.7) %, and 1.4 (2.4) %. There was no overshoot in venous occlusion, averaging at -1.2 (2.7) %; see Table 3. A significant difference in TSI_{Overshoot} was found for the resting conditions as well as venous occlusion with arterial occlusion; see Table 4. TSI_{Overshoot} in dynamic conditions averaged 11.8 (6.4) %, 9.6 (5.7) %, and 10.3 (5.8) % for Lucy, Paexo Shoulder, and Skelex 360.

A significant change in TSI_{Overshoot} was revealed between resting and dynamic conditions (movement) but not between pHMI design conditions or the interaction between pHMI design and movement by the multifactorial ANOVA; see Table 5.

4. Discussion

Safety will be the underlying evaluation criterion for future exoskeletons. Evaluation methods such as force, pressure, or subjective user experience assessment are insufficient or show inconsistencies, making safety regulations difficult to draw [50]. The underlying idea of this paper was to establish an additional safety criterion for pHMI designs and to capture tissue oxygenation as a physiological metric and direct physical effect of pHMI pressure.

Therefore, the study verified whether the use of circular interfaces of shoulder exoskeletons had an influence on tissue oxygenation and whether assisted movement with exoskeleton neutralizes a possible influence.

The comparison with the standard Vascular Occlusion Tests was chosen to verify whether occlusion also occurs due to the circular pressure of the pHMI or whether the TSI behavior differed systematically between VOT and exoskeleton conditions at rest. It can be assumed that a decrease in oxygen saturation during standard occlusion is a sign of venous blood stasis and that there is reduced blood flow in the capillary bed as a whole [51].

A sign of venous blood stasis is significant regarding two aspects. First, a reduced blood flow results in a reduced supply to the muscles and thus a reduced metabolic activity, which in turn can lead to painful and hardened muscles [52]. Second, a reduced blood flow favors the accumulation of platelets [53] which in turn can lead to thrombosis or embolism in a longer term. Because blood flow to the upper extremity is already reduced when the arms are elevated [25,27,32], additional occlusion through a shoulder exoskeleton interface becomes even more important.

4.1. Pressure

In the current study, subjects tightened the arm interface of the exoskeletons in such a way that the pressure of the pHMI was perceived as comfortable and the exoskeleton was easy to control, just as they would if the exoskeleton were in normal working use. The pressures within the Lucy and Skelex 360 interface are distinctively lower than the venous occlusion pressure, while the pressure within the Paexo Shoulder interface is not significantly different from the venous occlusion pressure (Table 3). With both Paexo Shoulder and Skelex 360, most study participants closed the interface to such an extent that both the threshold for initial venous occlusion (29.3 mmHg) [54] and the recommended threshold for exoskeletal interface pressure (20 mmHg) [39] were exceeded, which is in line with [40].

Mean pressure values increased in the dynamic use of the exoskeleton on average for 66%, 69%, and 61% in Lucy, Paexo Shoulder, and Skelex 360, respectively. This increase in

pressure is likely attributed to the displacement of the muscle belly during the movement and the change in muscle tone during the experimental task or the relative displacement between exoskeletal and biological interface components [15,55].

The pressure used by the subjects to tighten the Paexo Shoulder and Lucy exoskeleton interface differed systematically from one another (Table 4). The fact that the interface and the kinematics of these exoskeletons differ greatly could be of relevance here. The hard parts of the interface of the Paexo Shoulder exoskeleton enclose the arm to a greater extent (Table 2), while the arm rather rests on the hard part of the Lucy interface. In addition, subjects might have tightened the pHMI of the Paexo Shoulder using higher pressure to achieve enhanced control over the exoskeleton with its open kinematic chain and variable pivot point of the shoulder equivalent joints.

4.2. Tissue Oxygenation in Resting Position

When the TSI trajectories are visually inspected in exoskeleton conditions (Figure 7), initially there is a slight increase in TSI before there is a decrease in the values over the entire occlusion. After reopening the interfaces, TSI increases and a small overshoot occurs. The slight increase in TSI at the beginning of occlusion may be due to small movements of the subjects when the pHMIs were closed by the investigator.

TSI_{Slope1} showed no significant difference between the exoskeletal under resting conditions and venous occlusion (Table 4). Therefore, it can be concluded that hypothesis (i) can be confirmed. The low pressures within the exoskeletal interfaces already lead to restricted blood drainage following a reduction of oxygen saturation in the tissue underneath the interfaces, comparable to a two-minute standard venous occlusion at 50 mmHg.

The gradient of TSI_{Slope1} itself appears to depend predominantly on physiological processes, such as metabolic and oxygen consumption, since there was also no significant difference in the decrease in TSI_{Slope1} during the short occlusion period between arterial, venous, and exoskeletal occlusion.

TSI_{Slope2} and $TSI_{Overshoot}$ are representative of the ability of the organism to respond to the occlusion, remove venous blood and metabolites, and reoxygenate the tissue. For this purpose, the body uses reactive hyperemia. Generally, the extent of reactive hyperemia depends on the duration of the preceding ischemia (the longer, the more severe) and the metabolic activity of the affected area. During prolonged ischemia (>30 s), the partial pressure of oxygen drops and vasoactive metabolites accumulate. These trigger local chemical dilation of the vessel upon reopening [56] (pp. 202–208).

TSI_{Slope2} and $TSI_{Overshoot}$ did not differ significantly between venous and exoskeletal conditions, further indicating that blood supply is impeded by the pHMIs pressure (Table 4). The putative pressure difference (Table 4) between the exoskeletal interfaces does not appear to significantly affect the steepness of resaturation after occlusion. Rather, the pressure threshold leading to a decrease in TSI appears to be well below the 50 mmHg used in venous occlusion. This is in agreement with the considerations of Casavola et al. [54], who defined a threshold as low as 29 mmHg for the first venous blood flow restrictions.

4.3. Tissue Oxygenation in Dynamic Arm Movement

Previously, it was assumed that exoskeleton-assisted arm movement could compensate for a negative effect on tissue oxygen saturation by regular loading and unloading at the interface, activating the cardiovascular system as well as the musculovenous pump. The metabolic effects on the TSI response were estimated to be negligible because the shoulder muscles performed the main work of the dynamic task and the upper arm muscles had to perform only minor stabilization functions.

When visually inspecting the TSI trajectories under motion and closed pHMIs (Figure 7), TSI first overshoots, drops rapidly after ~15 s in a wave-like manner, and settles at a level slightly above baseline value after ~1.5 min. After reopening the pHMIs, the signal increases rapidly and overshoots significantly higher than in resting exoskeleton or venous conditions but returns to baseline faster than in arterial occlusion in resting posture. This signal behav-

ior, especially the TSI recovery rate and overshoot after occlusion, is usually not observed in studies with light exercise; compare [49,57,58]. It may have occurred as a motion artifact when subjects inadvertently tried to assist the examiner in closing the pHMI and slightly tightened the upper arm muscles.

The results of the dynamic TSI measurements are not yet fully understood. Contrary to hypothesis (ii), the study showed that exercise does not neutralize oxygen saturation in the tissue as long as the pHMI is closed. TSI_{Slope1} dropped significantly steeper in the occlusion period with movement compared to the resting conditions and TSI_{Slope2} showing significantly higher growths as well as higher $TSI_{Overshoot}$ values with movements (compare Tables 3 and 5). On the other hand, hypothesis (ii) is supported by the fact that the TSI values settle at a balanced level after some time of occlusion during the light activity. The reason for this will be functional vasodilation of the anterior arteries and arterioles due to motion [56].

The steeper downslope during occlusion with exercise, compared to rest, could be explained by enhanced metabolic activity as well as persistent stasis due to pHMI pressure. It seems unlikely that the increase in blood pressure in the capillary bed (due to vasodilation) rises to an extent that the external restrictive occlusion of pHMI is exceeded. Accordingly, the pHMI does not allow the removal of venous blood and the metabolites. This is also supported by the upslope and overshoot behavior of TSI.

TSI_{Slope2} and $TSI_{Overshoot}$, as expressions of a hyperemic response, show significant results only for the factor movement, but are not determined by the factor pHMI design or the interaction between both; compare Table 5. Therefore, the steeper increase in TSI_{Slope2} and the higher percentage of $TSI_{Overshoot}$ when performed with exercise probably reflect a combination of functional and reactive hyperemia, caused by blood stasis, metabolite accumulation, and cardiovascular activity. However, the influence of movement on TSI_{Slope2} and $TSI_{Overshoot}$ cannot be quantified, since in this first pilot no testing was run with motion only. The faster decline to baseline can probably be explained by the increased cardiovascular activity due to exercise.

4.4. Considerations on the Design of pHMIs

Discomfort is a key factor that often negatively affects the user experience when wearing occupational exoskeletons [19,59,60]. The pressures occurring within circular pHMIs, which already result in mild stasis, may be one reason for the perceived discomfort, as multifactorial analysis showed no effect for differences in pHMI design nor the interaction between design and movement (Table 5). However, all circular pHMI designs showed decreased TSI values in resting posture and dynamic use of the exoskeletons, indicating a reduced blood flow, already in the short-term use. Although a direct comparison of a circular and an open pHMI design is yet to be realized, it should be considered whether a circular enclosure design of the interfaces at the upper extremities is necessary. Open pHMIs would prevent an occlusion effect of a circular interface.

To optimize the pHMI fit, a design approach could be to account for human anthropometric heterogeneity and changes in volume during movement by performing anthropometric studies specifically tailored to the body region of a certain interface with the aid of 3D shape analysis [55,61]. In a second step, it is necessary to ensure that interfaces remain in position, either through active control (active exoskeletons) [62,63] or biomechanical measurements of relative movements (passive exoskeletons) [50].

In the case of an exoskeletal concept with an open kinematic chain and variable pivot points, which makes greater control by the user unavoidable, at least the interface should be provided with a band whose elasticity takes into account the changes in the volume of the muscle bellies during movement. For this purpose, pressure thresholds should be established that take into account the perfusion situation below the interface and keep deformations at a minimum [31].

4.5. Limitations

Pressure measurement between soft tissue and the soft padding of the pHMI is generally a difficult matter as human soft tissue hampers the reliability of measurements [64]. The pneumatic sensor was chosen in order to apply a system that could be easily integrated into the different pHMIs, without destroying the integrity of the pHMI and reducing their comfort. Using this type of sensor should not have any impact on the NIRS outcomes, because the sensor is flat, soft, and does not take much further space in the interface. Nevertheless, it is difficult to generalize the occurring pressures and to infer the total circumferential pressure of the pHMI. Due to the locally defined measurement, both pressure peaks and lows may have been recorded. To directly relate circumferential pressures to NIRS outcomes, a measurement method directly within the interface structure itself, for example, using strain gauges, would be necessary.

Deep tissue oxygenation was monitored directly under the tourniquet or pHMI, respectively. The NIRS readings may have been influenced by the pressure of the tourniquet or pHMI on the NIRS optodes and the tissue since the tissue underneath the optodes was compressed and possibly slightly displaced during occlusion.

NIRS measurements in standard occlusions are usually performed on relaxed muscles in a supine or sitting position to minimize the hydrostatic effects and thus establish comparable baseline conditions in the circulatory system. Since measurements in a sitting or even lying position were not possible with the exoskeletons, the NIRS investigation was limited to the area underneath the arm interface, which is at heart level. However, it would have been important to see how oxygen saturation distal to the interface, for example, on the forearm or hand, would have reacted to the occlusions of the pHMI. More basic research while standing would be needed to obtain valid results for areas further distal.

The study sample size is relatively small with 12 subjects. The study population was chosen very specifically to guarantee high-quality NIRS signals through low participants ATT [41]. The generalizability of the data may be reduced due to these two issues. Nevertheless, the results indicate an effect that has not received much attention within exoskeleton research to date. For further studies dealing with the effects of exoskeleton interface pressure on blood supply, it will be worthwhile to increase the generalizability and impact by choosing a larger sample size and a more diverse study population.

4.6. Future Work

The results need further verification in a large-scale study to evaluate the influence of the factors revealed in this pilot study. Some factors to be mentioned in the context of measuring tissue oxygenation when using exoskeletons are the dependence of the movement speed and or heart frequency, as well as possible motion artifacts at the moment of closing the pHMI. Future NIRS studies have to take these dependencies into account.

To further assess exoskeletal interfaces, a long-term recording of the tissue oxygen saturation over a comparable time to the average wearing time of shoulder exoskeletons is required. It is unclear how the body responds to the relatively low pressure of pHMI in the long term, especially if the assisted movement is maintained with an exoskeleton or is intermittent, as it would be in real work shifts. Especially in long-term studies, additional qualitative measures such as comfort scales should be used to reliably demonstrate the relationship between pressure, tissue oxygenation, and comfort. In addition, a direct comparison should be made between circular and open interface designs. Furthermore, it is still unclear what effects occur distal to the pHMI, for example, on the forearm and hands. In order to consider the hydrostatic effects here, further basic research with occlusions in the standing position is needed.

5. Conclusions

Three shoulder exoskeleton interfaces with a circular design were analyzed in comparison to a standardized vascular occlusion test at rest and dynamic usage regarding the oxygen level of the tissue underneath the interface. Tissue oxygenation was deter-

mined to assess the physical effects of exoskeleton interfaces and to establish a measure of exoskeleton user safety in addition to pure mechanical outcome parameters such as force, pressure, and relative motion. Accordingly, this new measure focuses the user when assessing human–exoskeleton interaction and is ultimately able to protect the user from possible undesirable mechanical loads. Conclusions about the design of pHMI can also be drawn using this new measure.

In the present study, it could be shown that tissue oxygenation decreases while wearing the exoskeletons with circular pHMIs at rest, indicating a negative effect of the circular pHMIs on tissue oxygenation. Contrary to the second hypothesis that movement neutralizes the negative effects of pHMI pressure by activating the muscular pump and the regular loading and unloading at the interface, in dynamic use, the tissue oxygen decreases faster than in rest with the exoskeletons. Intense reoxygenation and hyperemia after pHMI opening reflects combined functional and reactive hyperemia indicating that metabolites and venous blood could not be removed while wearing the exoskeletons. However, the stabilization of tissue oxygen near baseline is incoherent. Further research is needed to clarify the data. The shape and width of the different pHMIs influence the pressures occurring within the interfaces, but they do not differ significantly with respect to the rate of reduction of tissue oxygen saturation, reoxygenation, or hyperemic effects.

When designing new interfaces, consideration should be given to whether the interfaces can remain open from the outset to avoid occlusion effects. Otherwise, anthropometric design approaches are to be favored and elastic belts should account for the pressure change in dynamic use. Moreover, pressure tissue oxygenation should be investigated as a standard for the consequences of external pressures and constant oxygenation of the tissue should be ensured. A pressure threshold taking into account the tissue oxygen content should be established as a new measure of safety for pHMI of exoskeletons.

Author Contributions: Conceptualization, C.L., B.R. and R.W.; methodology, C.L., B.R., R.E. and R.W.; software, C.L.; validation, C.L. and B.R.; formal analysis, C.L., B.R. and R.E.; investigation, C.L.; resources, R.W.; data curation, C.L.; writing—original draft preparation, C.L.; writing—review and editing, C.L., B.R., R.E. and R.W.; visualization, C.L. and B.R.; supervision, R.W. All authors have read and agreed to the published version of the manuscript.

Funding: This research received no external funding.

Institutional Review Board Statement: The pilot study was conducted according to the guidelines of the Declaration of Helsinki and was approved by the University Innsbruck Advisory Board for Ethical Issues in Scientific Research (58/2021) on 3 August 2021.

Informed Consent Statement: Informed consent was obtained from all subjects involved in the study. Written informed consent has been obtained from the participants to publish this paper.

Data Availability Statement: Publicly available datasets were analyzed in this study. This data can be found here: <https://1drv.ms/f/s!AsB0zVKku9o6h9VaNmwoBUOHdv-noA?e=aFamps> (access date: 18 September 2023).

Conflicts of Interest: The authors declare no conflict of interest with respect to the design of the study; in the collection; analyses; or interpretation of data; in the writing of the manuscript; or in the decision to publish.

References

1. da Costa, B.R.; Vieira, E.R. Risk Factors for Work-Related Musculoskeletal Disorders: A Systematic Review of Recent Longitudinal Studies. *Am. J. Ind. Med.* **2010**, *53*, 285–323. [[CrossRef](#)] [[PubMed](#)]
2. Bosch, T.; van Eck, J.; Knitel, K.; de Looze, M. The Effects of a Passive Exoskeleton on Muscle Activity, Discomfort and Endurance Time in Forward Bending Work. *Appl. Ergon.* **2016**, *54*, 212–217. [[CrossRef](#)] [[PubMed](#)]
3. Otten, B.; Weidner, R.; Linnenberg, C. Leichtgewichtige und Inhärent Biomechanisch Kompatible Unterstützungssysteme Für Tätigkeiten in Und Über Kopfhöhe. In Proceedings of the 2. Transdisziplinäre Konferenz “Technische Unterstützungssysteme, Die Die Menschen Wirklich Wollen”, Hamburg, Germany, 12–13 December 2016; pp. 495–505.

4. Ersoysal, S.; Hoffmann, N.; Ralfs, L.; Weidner, R. Towards a Modular Elbow Exoskeleton: Concepts for Design and System Control. In *Annals of Scientific Society for Assembly, Handling and Industrial Robotics 2021*; Springer: Berlin/Heidelberg, Germany, 2022; pp. 141–152. [[CrossRef](#)]
5. Yao, Z.; Linnenberg, C.; Argubi-Wollesen, A.; Weidner, R.; Wulfsberg, J.P. Biomimetic Design of an Ultra-Compact and Light-Weight Soft Muscle Glove. *Prod. Eng.* **2017**, *11*, 731–743. [[CrossRef](#)]
6. Maurice, P.; Ivaldi, S.; Babic, J.; Camernik, J.; Gorjan, D.; Schirrmeister, B.; Bornmann, J.; Tagliapietra, L.; Latella, C.; Pucci, D.; et al. Objective and Subjective Effects of a Passive Exoskeleton on Overhead Work. *IEEE Trans. Neural Syst. Rehabil. Eng.* **2020**, *28*, 152–164. [[CrossRef](#)] [[PubMed](#)]
7. Otten, B.; Weidner, R.; Argubi-Wollesen, A. Evaluation of a Novel Active Exoskeleton for Tasks at or above Head Level. *IEEE Robot. Autom. Lett.* **2018**, *3*, 2408–2415. [[CrossRef](#)]
8. Pacifico, I.; Aprigliano, F.; Parri, A.; Cannillo, G.; Melandri, I.; Sabatini, A.M.; Violante, F.S.; Molteni, F.; Giovacchini, F.; Vitiello, N.; et al. Evaluation of a Spring-Loaded Upper-Limb Exoskeleton in Cleaning Activities. *Appl. Ergon.* **2023**, *106*, 103877. [[CrossRef](#)]
9. De Bock, S.; Ampe, T.; Rossini, M.; Tassignon, B.; Lefeber, D.; Rodriguez-Guerrero, C.; Roelands, B.; Geeroms, J.; Meeusen, R.; De Pauw, K. Passive Shoulder Exoskeleton Support Partially Mitigates Fatigue-Induced Effects in Overhead Work. *Appl. Ergon.* **2023**, *106*, 103903. [[CrossRef](#)]
10. Schmalz, T.; Schändlinger, J.; Schuler, M.; Bornmann, J.; Schirrmeister, B.; Kannenberg, A.; Ernst, M. Biomechanical and Metabolic Effectiveness of an Industrial Exoskeleton for Overhead Work. *Int. J. Environ. Res. Public Health* **2019**, *16*, 4792. [[CrossRef](#)]
11. Schröter, F.; Weidner, R.; Dehmel, P.; Jakobsen, T.; Wulfsberg, J. Der Beflügelte Mensch—Gesteigerte Konzentration Durch Unterstützungssysteme in Der Produktion. In Proceedings of the 51. DGPs-Kongress “Psychologie gestaltet”, Frankfurt am Main, Germany, 15–20 September 2018.
12. Weidner, R.; Linnenberg, C.; Hoffmann, N.; Prokop, G.; Edwards, V. Exoskelette Für Den Industriellen Kontext: Systematisches Review Und Klassifikation. In *Dokumentation des 66. Arbeitswissenschaftlichen Kongresses TU Berlin—Digitaler Wandel, Digitale Arbeit, Digitaler Mensch*; GfA-Press: Dortmund, Germany, 2020.
13. Nguialem, C.; Raison, M.; Achiche, S. Motion Planning of Upper-Limb Exoskeleton Robots: A Review. *Appl. Sci.* **2020**, *10*, 7626. [[CrossRef](#)]
14. Kuber, P.M.; Rashedi, E. Product Ergonomics in Industrial Exoskeletons: Potential Enhancements for Workforce Efficiency and Safety. *Theor. Issues Ergon. Sci.* **2020**, *22*, 729–752. [[CrossRef](#)]
15. Yandell, M.B.; Quinlivan, B.T.; Popov, D.; Walsh, C.; Zelik, K.E. Physical Interface Dynamics Alter How Robotic Exosuits Augment Human Movement: Implications for Optimizing Wearable Assistive Devices. *J. Neuroeng. Rehabil.* **2017**, *14*, 40. [[CrossRef](#)] [[PubMed](#)]
16. Linnenberg, C.; Weidner, R.; Wulfsberg, J.P.; Klabunde, J. Entwicklungsansatz Für Physische Mensch-Technik-Schnittstellen von Exoskeletten. In *Proceedings of the Band zur Dritten Transdisziplinäre Konferenz “Technische Unterstützungssysteme, Die Die Menschen Wirklich Wollen, 11–12 December 2018”*; Weidner, R., Karafillidis, A., Eds.; Helmut-Schmidt-Universität: Hamburg, Germany, 2018; pp. 417–424.
17. Xiloyannis, M.; Alicea, R.; Georgarakis, A.M.; Haufe, F.L.; Wolf, P.; Masia, L.; Riener, R. Soft Robotic Suits: State of the Art, Core Technologies, and Open Challenges. *IEEE Trans. Robot.* **2022**, *38*, 1343–1362. [[CrossRef](#)]
18. Francisco, A.; Yoe, J.; Morales, R.; Torres, G.O.; De Jes, F.; Sorcia, V.; Rojas, A.C.; Aurelio, J.; Mendoza, B. Soft Exoskeletons: Development, Requirements, and Challenges of the Last Decade. *Actuators* **2021**, *10*, 166. [[CrossRef](#)]
19. Baltrusch, S.J.; van Dieën, J.H.; van Bennekom, C.A.M.; Houdijk, H. The Effect of a Passive Trunk Exoskeleton on Functional Performance in Healthy Individuals. *Appl. Ergon.* **2018**, *72*, 94–106. [[CrossRef](#)]
20. de Looze, M.P.; Bosch, T.; Krause, F.; Stadler, K.S.; O’Sullivan, L.W. Exoskeletons for Industrial Application and Their Potential Effects on Physical Work Load. *Ergonomics* **2015**, *59*, 671–681. [[CrossRef](#)]
21. Tamez-Duque, J.; Cobian-Ugalde, R.; Kilicarlan, A.; Venkatakrisnan, A.; Soto, R.; Contreras-Vidal, J.L. Real-Time Strap Pressure Sensor System for Powered Exoskeletons. *Sensors* **2015**, *15*, 4550–4563. [[CrossRef](#)]
22. Quinlivan, B.; Asbeck, A.; Wagner, D.; Ranzani, T.; Russo, S.; Walsh, C. Force Transfer Characterization of a Soft Exosuit for Gait Assistance. In Proceedings of the ASME 2015 International Design Engineering Technical Conferences & Computers and Information in Engineering Conference (IDETC/CIE 2015), Boston, MA, USA, 2–5 August 2015; 5A-2015; pp. 1–8. [[CrossRef](#)]
23. Agam, L.; Gefen, A. Pressure Ulcers and Deep Tissue Injury: A Bioengineering Perspective. *J. Wound Care* **2007**, *16*, 336–342. [[CrossRef](#)]
24. Bouten, C.V.; Oomens, C.W.; Baaijens, F.P.; Bader, D.L. The Etiology of Pressure Ulcers: Skin Deep or Muscle Bound? *Arch. Phys. Med. Rehabil.* **2003**, *84*, 616–619. [[CrossRef](#)]
25. Järholm, U.; Palmerud, G.; Karlsson, D.; Herberths, P.; Kadefors, R. Intramuscular Pressure and Electromyography in Four Shoulder Muscles. *J. Orthop. Res.* **1991**, *9*, 609–619. [[CrossRef](#)]
26. Charles, L.E.; Ma, C.C.; Burchfiel, C.M.; Dong, R.G. Vibration and Ergonomic Exposures Associated with Musculoskeletal Disorders of the Shoulder and Neck. *Saf. Health Work* **2018**, *9*, 125–132. [[CrossRef](#)]
27. Garg, A.; Hegmann, K.; Kapellusch, J. Short-Cycle Overhead Work and Shoulder Girdle Muscle Fatigue. *Int. J. Ind. Ergon.* **2006**, *36*, 581–597. [[CrossRef](#)]

28. Meier, T.O.; Tschirch, F.F.; Weisheupt, D.; Hug, U.; Giovanoli, P.; Schiller, A. Thoracic-Outlet-Syndrom (TOS). *gefaessmedizin.net* **2008**, *4*, 18–50. [[CrossRef](#)]
29. Buckle, P.; Devereux, J. The Nature of Work-Related Neck and Upper Limb Musculoskeletal Disorders. *Appl. Ergon.* **2002**, *33*, 207–217. [[CrossRef](#)] [[PubMed](#)]
30. Armstrong, T.; Buckle, P.; Fine, L.J.; Hagberg, M.; Jonsson, B.; Kilborn, A.; Kuorinka, I.A.A.; Silverstein, B.A.; Sjøgaard, G.; Viikari-juntura, E.R.A. A Conceptual Model for Work-Related Musculoskeletal Disorders Neck and Upper-Limb. *Scand. J. Work. Environ. Health* **1993**, *19*, 73–84. [[CrossRef](#)] [[PubMed](#)]
31. Oomens, C.W.J.; Loerakker, S.; Bader, D.L. The Importance of Internal Strain as Opposed to Interface Pressure in the Prevention of Pressure Related Deep Tissue Injury. *J. Tissue Viability* **2010**, *19*, 35–42. [[CrossRef](#)]
32. Weston, E.B.; Alizadeh, M.; Hani, H.; Knapik, G.G.; Souchereau, R.A.; Marras, W.S. A Physiological and Biomechanical Investigation of Three Passive Upper-Extremity Exoskeletons during Simulated Overhead Work. *Ergonomics* **2022**, *65*, 105–117. [[CrossRef](#)]
33. Muramatsu, Y.; Kobayashi, H. Assessment of Local Muscle Fatigue by NIRS—Development and Evaluation of Muscle Suit. *Robomech J.* **2014**, *1*, 19. [[CrossRef](#)]
34. Hefferle, M.; Lechner, M.; Kluth, K.; Christian, M. Development of a Standardized Ergonomic Assessment Methodology for Exoskeletons Using Both Subjective and Objective Measurement Techniques. In *Advances in Human Factors in Robots and Unmanned Systems, Proceedings of the AHFE 2016 International Conference on Human Factors in Robots and Unmanned Systems, Orlando, FL, USA, 27–31 July 2016*; Savage-Knepshield, P., Chen, J., Eds.; Springer: Berlin/Heidelberg, Germany, 2016; pp. 49–59, ISBN 978-3-319-41959-6.
35. Zhu, Y.; Weston, E.B.; Mehta, R.K.; Marras, W.S. Neural and Biomechanical Tradeoffs Associated with Human-Exoskeleton Interactions. *Appl. Ergon.* **2021**, *96*, 103494. [[CrossRef](#)]
36. Caliandro, P.; Molteni, F.; Simbolotti, C.; Guanzioli, E.; Iacovelli, C.; Reale, G.; Giovannini, S.; Padua, L. Exoskeleton-Assisted Gait in Chronic Stroke: An EMG and Functional near-Infrared Spectroscopy Study of Muscle Activation Patterns and Prefrontal Cortex Activity. *Clin. Neurophysiol.* **2020**, *131*, 1775–1781. [[CrossRef](#)]
37. Kermavnar, T.; O’Sullivan, K.J.; de Eyto, A.; O’Sullivan, L.W. Discomfort/Pain and Tissue Oxygenation at the Lower Limb During Circumferential Compression: Application to Soft Exoskeleton Design. *Hum. Factors* **2020**, *62*, 475–488. [[CrossRef](#)]
38. Kermavnar, T.; O’Sullivan, K.J.; Casey, V.; de Eyto, A.; O’Sullivan, L.W. Circumferential Tissue Compression at the Lower Limb during Walking, and Its Effect on Discomfort, Pain and Tissue Oxygenation: Application to Soft Exoskeleton Design. *Appl. Ergon.* **2020**, *86*, 103093. [[CrossRef](#)]
39. Schiele, A.; van der Helm, F.C.T. Influence of Attachment Pressure and Kinematic Configuration on PHRI with Wearable Robots. *Appl. Bionics Biomech.* **2009**, *6*, 157–173. [[CrossRef](#)]
40. Linnenberg, C.; Weidner, R. Industrial Exoskeletons for Overhead Work: Circumferential Pressures on the Upper Arm Caused by the Physical Human-Machine-Interface. *Appl. Ergon.* **2022**, *101*, 103706. [[CrossRef](#)]
41. van Beekvelt, M.C.P.; Borghuis, M.S.; van Engelen, B.G.M.; Wevers, R.A.; Colier, W.N.J.M. Adipose Tissue Thickness Affects in Vivo Quantitative Near-IR Spectroscopy in Human Skeletal Muscle. *Clin. Sci.* **2001**, *101*, 21–28. [[CrossRef](#)]
42. Barstow, T.J. Understanding near Infrared Spectroscopy and Its Application to Skeletal Muscle Research. *J. Appl. Physiol.* **2019**, *126*, 1360–1376. [[CrossRef](#)]
43. Patterson, M.S.; Chance, B.; Wilson, B.C. Time Resolved Reflectance and Transmittance for the Non-Invasive Measurement of Tissue Optical Properties. *Appl. Opt.* **1989**, *28*, 2331–2336. [[CrossRef](#)]
44. van der Zee, P.; Cope, M.; Arridge, S.R.; Essenpreis, M.; Potter, L.A.; Edwards, A.D.; Wyatt, J.S.; McCormick, D.C.; Roth, S.; Reynolds, E.O.R. Experimentally Measured Optical Pathlengths for the Adult Head, Calf and Forearm and the Head of the Newborn Infant as a Function of Inter Optode Spacing. *Adv. Exp. Med. Biol.* **1992**, *316*, 143–153.
45. Ferrari, M.; Wei, Q.; Carraresi, L.; De Blasi, R.A.; Zaccanti, G. Time-Resolved Spectroscopy of the Human Forearm. *J. Photochem. Photobiol. B* **1992**, *16*, 141–153. [[CrossRef](#)]
46. Bezemer, R.; Lima, A.; Myers, D.; Klijn, E.; Heger, M.; Goedhart, P.T.; Bakker, J.; Ince, C. Assessment of Tissue Oxygen Saturation during a Vascular Occlusion Test Using Near-Infrared Spectroscopy: The Role of Probe Spacing and Measurement Site Studied in Healthy Volunteers. *Crit. Care* **2009**, *13* (Suppl. S5), 244. [[CrossRef](#)]
47. Futier, E.; Christophe, S.; Robin, E.; Petit, A.; Pereira, B.; Desbordes, J.; Bazin, J.E.; Vallet, B. Use of Near-Infrared Spectroscopy during a Vascular Occlusion Test to Assess the Microcirculatory Response during Fluid Challenge. *Crit. Care* **2011**, *15*, R214. [[CrossRef](#)]
48. Payen, D.; Luengo, C.; Heyer, L.; Resche-Rigon, M.; Kerever, S.; Damoiseil, C.; Lossner, M.R. Is Thenar Tissue Hemoglobin Oxygen Saturation in Septic Shock Related to Macrohemodynamic Variables and Outcome? *Crit. Care* **2009**, *13* (Suppl. S5), S6. [[CrossRef](#)]
49. Jones, S.; Tillin, T.; Williams, S.; Rapala, A.; Chaturvedi, N.; Hughes, A.D. Skeletal Muscle Tissue Saturation Changes Measured Using Near Infrared Spectroscopy during Exercise Are Associated with Post-Occlusive Reactive Hyperaemia. *Front. Physiol.* **2022**, *13*, 919754. [[CrossRef](#)]
50. Massardi, S.; Rodriguez-Cianca, D.; Pinto-Fernandez, D.; Moreno, J.C.; Lancini, M.; Torricelli, D. Characterization and Evaluation of Human-Exoskeleton Interaction Dynamics: A Review. *Sensors* **2022**, *22*, 3993. [[CrossRef](#)]
51. De Blasi, R.A.; Ferrari, M.; Natali, A.; Conti, G.; Mega, A.; Gasparetto, A. Noninvasive Measurement of Forearm Blood Flow and Oxygen Consumption by Near-Infrared Spectroscopy. *J. Appl. Physiol.* **1994**, *76*, 1388–1393. [[CrossRef](#)]

52. Hach, W. *VenenChirurgie: Operative, Interventionelle und Konservative Aspekte*, 3rd ed.; Schattauer: Stuttgart, Germany, 2013; ISBN 9783794528424.
53. Packer, C.F.; Bickel, S.; Dattilo, J.B. *Vein Obstruction*; StatPearls Publishing: Tampa, FL, USA, 2023.
54. Casavola, C.; Paunescu, L.A.; Fantini, S.; Gratton, E. Blood Flow and Oxygen Consumption with Near-Infrared Spectroscopy and Venous Occlusion: Spatial Maps and the Effect of Time and Pressure of Inflation. *J. Biomed. Opt.* **2000**, *5*, 269. [[CrossRef](#)]
55. Linnenberg, C.; Weidner, R. Designing Physical Human-Machine-Interfaces for Exoskeletons Using 3D-Shape Analysis. In Proceedings of the 3DBODY.TECH 2019—10th International Conference and Exhibition on 3D Body Scanning and Processing Technologies, Lugano, Switzerland, 22–23 October 2019; pp. 85–95.
56. Klinker, R. *Physiologie*; Georg Thieme Verlag: Stuttgart, Germany, 2005; ISBN 9783131924353.
57. McManus, C.J.; Collison, J.; Cooper, C.E. Performance Comparison of the MOXY and PortaMon Near-Infrared Spectroscopy Muscle Oximeters at Rest and during Exercise. *J. Biomed. Opt.* **2018**, *23*, 1. [[CrossRef](#)]
58. van Hooff, M.; Meijer, E.J.; Scheltinga, M.R.M.; Savelberg, H.H.C.M.; Schep, G. Test–Retest Reliability of Skeletal Muscle Oxygenation Measurement Using near-Infrared Spectroscopy during Exercise in Patients with Sport-Related Iliac Artery Flow Limitation. *Clin. Physiol. Funct. Imaging* **2022**, *42*, 114–126. [[CrossRef](#)]
59. Baldassarre, A.; Lulli, L.G.; Cavallo, F.; Fiorini, L.; Mariniello, A.; Mucci, N.; Arcangeli, G. Industrial Exoskeletons from Bench to Field: Human-Machine Interface and User Experience in Occupational Settings and Tasks. *Front. Public Health* **2022**, *10*, 1039680. [[CrossRef](#)]
60. de Looze, M.P.; Krause, F.; O’Sullivan, L.W. The Potential and Acceptance of Exoskeletons in Industry. In *Wearable Robotics: Challenges and Trends*; González-Vargas, J., Ibáñez, J., Contreras-Vidal, J., van der Kooij, H., Pons, J., Eds.; Springer: Berlin/Heidelberg, Germany, 2017; pp. 195–199.
61. Perry, J.C.; Brower, J.R.; Carne, R.H.R.; Bogert, M.A. 3D Scanning of the Forearm for Orthosis and HMI Applications. *Front. Robot. AI* **2021**, *8*, 576783. [[CrossRef](#)]
62. Baud, R.; Manzoori, A.R.; Ijspeert, A.; Bouri, M. Review of Control Strategies for Lower-Limb Exoskeletons to Assist Gait. *J. Neuroeng. Rehabil.* **2021**, *18*, 1–34. [[CrossRef](#)]
63. Aguirre-Ollinger, G.; Colgate, J.E.; Peshkin, M.A.; Goswami, A. Active-Impedance Control of a Lower-Limb Assistive Exoskeleton. In Proceedings of the 2007 IEEE 10th International Conference on Rehabilitation Robotics, Noordwijk, The Netherlands, 13–15 June 2007; pp. 188–195. [[CrossRef](#)]
64. Levesque, L.; Pardoel, S.; Doumit, M.; Lovrenovic, Z. Experimental Comfort Assessment of an Active Exoskeleton Interface. In Proceedings of the IEEE International Symposium on Robotics and Intelligent Sensors (IRIS), Ottawa, ON, Canada, 5–7 October 2017; pp. 5–7.

Disclaimer/Publisher’s Note: The statements, opinions and data contained in all publications are solely those of the individual author(s) and contributor(s) and not of MDPI and/or the editor(s). MDPI and/or the editor(s) disclaim responsibility for any injury to people or property resulting from any ideas, methods, instructions or products referred to in the content.